The Role of Deformation and Other Quantities in an Equation for Enstrophy as Applied to Atmospheric Blocking

Andrew D. Jensen, Anthony R. Lupo

Department of Soil, Environmental, and Atmospheric Sciences, 302 Anheuser Busch Natural Resources Building, University of Missouri, Columbia, MO, 65211.

Abstract

In this note, equations for enstrophy and enstrophy advection are derived in terms of well-known quantities, assuming horizontal frictionless flow on a beta-plane. Specifically, enstrophy can be written in terms of the geopotential (or pressure), relative vorticity, zonal wind, and resultant deformation. Enstrophy advection is shown to be related to the time evolution of deformation and ageostrophic relative vorticity. Based on previous research, these terms may contribute to instability associated with atmospheric blocking development and decay.

Keywords: blocking anticyclone, stability theory, enstrophy

1.

Studies have shown that the onset and decay periods of blocking are characterized by flow instability, (Haines and Holland [4], Hansen and Sutera [5]). Moreover, recent work suggests that blocking regime transition can be detected by means of certain enstrophy based diagnostics, which may be used to assess the stability changes in the flow that lead to atmospheric blocking regime transition, (e.g. Dymnikov *et al.* [2]). In particular, Athar and Lupo [1], Jensen and Lupo [6, 7], Lupo *et al.* [11, 12] used changes in instability and instability maxima at block onset and decay to detect blocking regime transition with two related enstrophy based diagnostic quantities. However,

Email address: jensenad@missouri.edu (Andrew D. Jensen)

a sufficient physical explanation for the diagnostics introduced in Lupo *et al.* [11], Jensen and Lupo [6] was not given.

The method employed here is to derive an equation for enstrophy to show that enstrophy (assuming frictionless flow on a beta-plane) can be written in terms of the geopotential (or pressure), relative vorticity, zonal wind, and resultant deformation. Furthermore, to emphasize the importance of the deformation term in the equation, a phase relation and solution of the enstrophy equation in idealized situations are found. Next, to illustrate the correctness of the enstrophy equation, the terms in the equation are calculated from reanalysis data for a strong blocking event and their magnitudes are compared to determine their relative importance in the enstrophy budget. The resultant deformation was found to be largest in magnitude throughout the blocking event and thus to contribute most to the instability at block onset and decay. Finally, enstrophy advection can be shown to be equal to the time evolution of the deformation and the ageostrophic advection of ageostrophic vorticity; relationships between these two quantities are examined.

The importance of this work is that based on previous research, the enstrophy diagnostics described below appear to introduce necessary conditions for blocking regime transition and the quantities that make up the equations derived below contribute to instability as described by the diagnostics. Since the diagnostics behave as expected for all events studied in past research (Athar and Lupo [1], Jensen and Lupo [6, 7], Lupo *et al.* [11, 12]), further investigation of these diagnostics appears to be justified.

The outline of this paper is as follows. In section 2 we present the stability diagnostics to be used. In section 3 we present the equations and approximate solutions to offer physical explanations in idealized situations. Moreover, the terms in the enstrophy equation are calculated and the magnitudes compared. In section 4 we discuss our findings and summarize our conclusions.

2. Diagnostics

As demonstrated in Dymnikov *et al.* [2] and Jensen and Lupo [7], the sum of the finite-time Lyapunov exponents for the barotropic vorticity equation may be approximated by the integral of enstrophy, called IRE hereafter, where the integral is evaluated over an entire hemisphere, i.e.,

$$\sum_{\lambda_i>0} \lambda_i \approx \int \zeta^2 \mathrm{d}A,$$

where λ_i are the finite-time Lyapunov exponents, ζ is the relative vorticity, and the integral is taken over the 500 hPa surface. In Athar and Lupo [1], Jensen and Lupo [6, 7], Lupo *et al.* [11, 12] these ideas were implemented to identify blocking regime transition by means of the following diagnostic quantities,

$$IRE := \int \zeta^2 \mathrm{d}A \tag{1}$$

$$DIRE := -\int \mathbf{v}_h \cdot \nabla_h \zeta^2 \mathrm{d}A = -\int \nabla_h \cdot \left(\mathbf{v}_h \zeta^2\right) \mathrm{d}A, \tag{2}$$

where the DIRE is the derivative of the IRE assuming frictionless non-divergent barotropic flow on an f-plane. In these studies, the IRE was observed to increase to local maxima during the block development and decay stages, indicating a local instability maximum in the flow. The local maxima of the IRE at onset and decay of blocking are used as diagnostics of blocking regime transition. The IRE has been used to examine blocking events in both hemispheres. From (2) and the divergence theorem, the DIRE can be thought of as the enstrophy flux across a boundary in the flow. Jensen and Lupo [6] showed that the DIRE is a useful diagnostic to detect blocking regime transition by using the sign of the integral to determine changes in instability. In Jensen and Lupo [6, 7] enstrophy advection changing signs from positive (increasing instability) to negative (decreasing instability) was used to as a diagnostic for the transition from blocked (unblocked) to unblocked (blocked) flow.

While the IRE and DIRE do not unambiguously identify blocking, since they behave as described for all events studied in (Athar and Lupo [1], Jensen and Lupo [6], Lupo *et al.* [11, 12]), which include over three years of events, they appear to demonstrate a necessary behavior for block onset and decay.

If the hypothesis of frictionless flow is dropped and we start with the barotropic vorticity equation in the form

$$\frac{\mathrm{d}}{\mathrm{d}t}\zeta = \frac{1}{R}\nabla_h^2 \zeta,$$

where R is the Reynolds number, then

$$\frac{\mathrm{d}}{\mathrm{d}t}\int \zeta^2 \mathrm{d}A = -\frac{2}{R}\int \left(\nabla_h \zeta\right)^2 \mathrm{d}A, \tag{3}$$

(see Pedlosky [13] chapter 4). The stability implied by (3) may hold at times between block onset and decay. For large Reynolds numbers on the other hand (as $R \longrightarrow \infty$) and if $(\nabla\zeta)^2$ stays bounded then (see (2)) the friction term may be ignored in the free atmosphere. This may apply especially at block onset and decay.

3. Results

3.1. Enstrophy Equation

In this section we derive an equation for enstrophy to determine the physical quantities that contribute to the instability at block onset and decay as indicated by the IRE (see (1)). To that end, by taking the divergence of the frictionless horizontal equations of motion

$$\frac{\mathrm{d}\mathbf{v}_h}{\mathrm{d}t} = -\nabla_h\phi - f\mathbf{k}\times\mathbf{v}_h,$$

it can be shown that

$$\nabla_h^2\phi - f\zeta + \beta u = 2J(u,v), \tag{4}$$

where ∇_h^2 is the horizontal Laplacian, J is the Jacobian determinant, ϕ is the geopotential, and ζ is the relative vorticity. Only horizontal frictionless flow, $\nabla_h\cdot\mathbf{v}_h = 0$, and $f = f_0 + \beta y$ have been assumed here. Straightforward manipulation using $\nabla_h\cdot\mathbf{v}_h = 0$ yields the identity

$$\frac{1}{2}\left(\zeta^2 - \sigma^2\right) = 2J(u,v), \tag{5}$$

where $\sigma^2 = (\partial_x u - \partial_y v)^2 + (\partial_x v + \partial_y u)^2$, and consists of stretching and shearing deformation. For brevity, we call it simply deformation in this note. See Weiss [16] for an explanation of the importance of these ideas in a non-rotating system. By putting equations (4) and (5) together the following equation for the enstrophy holds

$$\frac{1}{2}\zeta^2 = \nabla_h^2\phi - f\zeta + \beta u + \frac{1}{2}\sigma^2. \tag{6}$$

We note that if there is significant cancellation between $\nabla_h^2\phi$ and $f\zeta$ (as in geostrophy) then (6) reduces to

$$\frac{1}{2}\zeta^2 = \beta u + \frac{1}{2}\sigma^2.$$

In this situation the deformation can then be written in terms of its dimensions as

$$\sigma^2 \sim \frac{U^2 - 2\beta U L^2}{L^2},$$

where again U, L are characteristic velocity and length scales. When $U > 0$, there is a small decrease in deformation. On the other hand, if $U < 0$, or where there is a weakening of the westerlies (see Dong and Colucci [3]) as in blocking, there is a small increase in deformation.

3.2. Particular solution

To emphasize the importance of deformation in blocking events a particular solution of the deformation field in an idealized situation is found and shown to be related to the geopotential. To that end we assume an inviscid barotropic flow. By multiplying the barotropic vorticity equation by ζ,

$$\frac{1}{2}\frac{\mathrm{d}\zeta^2}{\mathrm{d}t} = -\beta v \zeta,$$

where v is the meridional component of the wind. Using this, $\frac{\mathrm{d}}{\mathrm{d}t}$(6) results in

$$0 = \frac{\mathrm{d}\nabla_h^2 \phi}{\mathrm{d}t} + f v \beta + \beta \frac{\mathrm{d}u}{\mathrm{d}t} + \frac{1}{2}\frac{\mathrm{d}\sigma^2}{\mathrm{d}t},$$

or

$$C = \nabla_h^2 \phi + f_0 \beta y + \beta u + \frac{1}{2}\sigma^2,$$

where $f\beta y \approx f_0 \beta y$ has been used. C is a constant which, if 0 initially is always 0. For simplicity C is assumed equal to zero; geostrophy is also assumed. Further, the term $f_0 \beta y$ may be ignored if the scale is small enough ($\sim 10^4$m). That is, a portion of the block can be considered such as part of the western edge in the Northern Hemisphere where there is the characteristic split flow in blocking events. Then, the following equation is obtained:

$$0 = \nabla_h^2 \phi - \frac{\beta}{f_0}\partial_y \phi + \frac{1}{2}\sigma^2(\phi). \tag{7}$$

By Taylor expanding the composite function $\sigma^2(\phi)$ in ϕ, retaining only the linear part $\sigma^2(\phi) \approx A_0 + A\phi$, where A_0, A are constants, and assuming $A_0 = 0$ for simplicity, (7) becomes

$$\nabla_h^2 \phi - \frac{\beta}{f_0}\partial_y \phi + \frac{A}{2}\phi = 0.$$

If A_0 is not assumed equal to 0, this equation can still be solved, but not necessarily in closed form. This equation has particular solution (see Figure 1 for contours)

$$\phi(x,y,t) = 2e^{\frac{\beta y}{2f_0}} \cosh\left(\frac{y}{2}\sqrt{\left(\frac{\beta}{f_0}\right)^2 - 2A + 4k^2} \right) \cos(kx). \tag{8}$$

Hence to first order, the deformation (or ϕ) is determined by (8).

Again, consider

$$\nabla_h^2\phi + f_0\beta y - \frac{\beta}{f_0}\partial_y\phi + \frac{A}{2}\phi = 0,$$

where the term $f_0\beta y$ is retained. Assuming a simple wave solution of the form $\phi = \cos\left(kx + ly + \omega t\right)$ and substituting ϕ into the equation above,

$$-\left(k^2 + l^2\right)\phi + \frac{\beta k}{\omega}\phi + \frac{\beta l}{f_0}\sin\left(kx + ly + \omega t\right) + \frac{A}{2}\phi = 0.$$

Since blocking is a midlattitude phenomenon, $\phi \approx \sin\left(kx + ly + \omega t\right)$ so that we have

$$-\left(k^2 + l^2\right) + \frac{\beta k}{\omega} + \frac{\beta l}{f_0} + \frac{A}{2} = 0.$$

By simplifying the previous equation the following dispersion relation is obtained:

$$\omega = \frac{2f_0\beta k}{2f_0(k^2 + l^2) - 2\beta l - Af_0},$$

(see Figure 2).

3.3. General Case

More generally, the full divergence equation can be considered,

$$\frac{\mathrm{d}D}{\mathrm{d}t} + D^2 + \nabla_h\omega \cdot \partial_p\mathbf{v}_h - \mathbf{k}\cdot\left(\nabla_h \times (f\mathbf{v}_h)\right) = -\nabla^2\phi + 2J(u,v), \tag{9}$$

where $D = \partial_x u + \partial_y v$. Straightforward calculations (assuming $f = f_0 + \beta y$ and $\nabla \cdot \mathbf{v}_h = -\partial_p\omega$) similar to those leading to (6) yield

$$\frac{1}{2}\left(\zeta^2 - \sigma^2\right) = \frac{\mathrm{d}D}{\mathrm{d}t} + \nabla^2\phi - f\zeta + u\beta + \frac{1}{2}\left(\partial_p\omega\right)^2 + \nabla_h\omega \cdot \partial_p\mathbf{v}_h. \tag{10}$$

When the continuity equation is given by $\nabla \cdot \mathbf{v}_h = -\partial_p \omega$, (i.e. the motions are not purely horizontal as before) the equation for enstrophy takes into account more physical quantities. In particular, the important effects of divergence and vertical motions are shown to play a role in the instability at block onset and decay and the maintenance of the enstrophy budget. We note that this case reduces to (6) when $\nabla \cdot \mathbf{v}_h = 0$.

3.4. IRE from Equation (6)

To illustrate the accuracy and correctness of equation (6), the NCEP/NCAR gridded reanalysis data set (Kalnay *et al.* [8]) is used to calculate the IRE from (6). The magnitudes of the terms in (6) were calculated to illustrate the important quantities that lead to instability as described by (1) and (2), (see Figure 4). The 0000 UTC NCEP/NCAR reanalyses of gridded (2.5-degree) 500 hPa u, v components of the wind and 500 hPa geopotential heights were used in the calculations of the terms in (6). The blocking definition given in Lupo and Smith [10] (see Appendix) was used to determine the times of block onset and decay for the event from 25 March to 2 April 2012, (see Figure 3). The block was centered at 0 E at onset and had a blocking intensity (BI) of 5.06 making it a strong event, where the blocking intensity, as introduced in Wiedenmann *et al.* [17], describes the strength of the blocking event. For the blocking event described above, the right-hand side of equation (6) was integrated over the Northern Hemisphere to calculate the IRE and was compared to the IRE calculated by means of the integral of enstrophy alone in order to illustrate the contribution of the terms to the enstrophy budget. The calculations were done from May 23 to April 4 2012, to show the development a few days before and after the blocking event. The IRE as calculated from (6) is in reasonable agreement with the IRE calculated alone, (see Figure 4), where the highest relative error is $\sim 10\%$ around May 30th (see Figure 4), while the other relative errors are much smaller. It can be seen that the the IRE increases sharply at block onset and reaches a relative maximum at decay. The time series of the magnitudes of the terms in (6) for the blocking event are shown in Figure 4. In this case, the deformation has the largest magnitude throughout the event, and the relative vorticity increases in magnitude after block onset, which is consistent with the dynamics of blocking, (see Lupo and Smith [10]).

3.5. Enstrophy Advection

Now, taking $\frac{\partial}{\partial t}(6)$ results in

$$-\mathbf{v}_h \cdot \nabla_h \zeta^2 = 2\beta v \zeta + 2f \mathbf{v}_{ag} \cdot \nabla \zeta_{ag} + 2f v_{ag} \beta + 2\beta \partial_t u + \partial_t \sigma^2, \qquad (11)$$

where a frictionless, non-divergent barotropic flow on a beta-plane has been assumed.

In Jensen and Lupo [6], an f-plane was assumed in order to obtain the DIRE diagnostic. If $f \approx f_0$, then

$$-\mathbf{v}_h \cdot \nabla_h \zeta^2 = 2f_0 \mathbf{v}_{ag} \cdot \nabla \zeta_{ag} + \partial_t \sigma^2. \qquad (12)$$

Hence, the enstrophy advection is distributed between the time evolution of the deformation and the advection of ageostrophic vorticity by the ageostrophic wind. When $2f_0 \mathbf{v}_{ag} \cdot \nabla \zeta_{ag} \ll -\mathbf{v}_h \cdot \nabla_h \zeta^2, \partial_t \sigma^2$, then

$$\partial_t \sigma^2 = -\nabla_h \cdot \left(\mathbf{v}_h \zeta^2 \right).$$

By the divergence theorem

$$\frac{\partial}{\partial t} \int \sigma^2 dA = \oint_C \zeta^2 \mathbf{v}_h \cdot \mathbf{n} ds,$$

where C is a fluid boundary.

On the other hand, if the ageostrophic terms cannot be ignored, then as mentioned in section 2, when the IRE achieves a local maximum value (local maximum instability is implied) it follows that,

$$\partial_t \sigma^2 + 2f_0 \mathbf{v}_{ag} \cdot \nabla \zeta_{ag} = 0. \qquad (13)$$

Under these assumptions the local time rate of change of deformation can be described as advection by the ageostrophic wind of the ageostrophic vorticity. Now, we suppose that there exists a streamfunction

$$\psi_{ag}(x, y, t) = \cos(ly) \sin(kx - \omega t) \qquad (14)$$

describing the ageostrophic motions. Then it follows by substituting (14) into (13) that $\partial_t \sigma^2 = 0$, that is, σ^2 is steady state, or locally constant. Other streamfunctions describing the ageostrophic motions can be found of the form

$$\psi_{ag}(x, y, t) = A(y) \sin(kx - \omega t)$$

and yielding the same result such as one with $A(y) = By + C$, where B, C are constants. We note that an analysis could be performed similar to that in section 3.4. However, blocking events evolve on a time scale of days and hence the time derivatives in (12) are crude estimates. We therefore omit such an analysis in this paper

4. Discussion and Conclusions

It has been shown that enstrophy and enstrophy advection can be written in terms involving the geopotential, relative vorticity, zonal wind, and deformation, assuming only horizontal frictionless flow on a beta-plane. These quantities have been shown to be important in blocking, (see e.g. Dong and Colucci [3], Lupo and Smith [10]). Assuming frictionless, barotropic flow on a beta-plane, the enstrophy advection was shown to be equal to the time evolution of the deformation and the ageostrophic advection of ageostrophic vorticity. In particular, we have shown that based on previous results Dymnikov *et al.* [2], Jensen and Lupo [6, 7], Lupo *et al.* [11] the terms in both equations derived here may contribute to the instability associated with blocking onset and decay and provide insight into the ways in which the diagnostic quantities introduced in these studies may be used to identify blocking regime transition. An example of a calculation of the terms in the enstrophy equation compared to enstrophy alone was provided. There was reasonable agreement between the two, as expected from the theory. The small differences in values may be a result of the course data set, round-off error, the non-linearities in the equation, neglected friction, etc. The deformation term has the largest magnitude for each calculation time. This may imply that it contributes most to the instability implied by the diagnostics. The relative vorticity mostly increases from onset until decay. We note that we have neglected friction because of the turbulent nature of block onset and decay, and also because frictional effects tend to be small at 500 hPa in the atmosphere. We also note that, although the results have been framed in terms of atmospheric blocking, the results can be generalized to and may be of interest in other atmospheric situations. Appropriate terms could be introduced in (6) and (12) to account for friction.

The terms in (6) were calculated from reanalysis data for a strong blocking event and their magnitudes compared to determine their relative importance in the enstrophy budget. It is not practical to calculate the IRE from (6) or the DIRE from (12). Rather the importance of the equations is to illustrate the quantities that contribute to instability as indicated by (1) and (2). It is important to point again out that the diagnostics explored in this paper do not unambiguously define block onset and decay. However, for all events studied in Athar and Lupo [1], Jensen and Lupo [6, 7], Lupo *et al.* [11, 12] and based on the idea that the flow is unstable at onset and decay (see Haines and Holland [4], Hansen and Sutera [5]), the diagnostics seem to give a necessary condition of a maximum in IRE at block onset (decay) and DIRE changing from positive to negative at onset (decay). The local IRE maximum appears to be heavily influenced by deformation, increasing relative vorticity compared to the other terms in equation (6). The DIRE change may come about by way of ageostrophic advections of the ageostrophic vorticity.

Acknowledgements

We express our thanks to the reviewers for their helpful comments and suggestions which strengthened the presentation of our results.

Appendix A.

Briefly, the blocking criterion used here includes (i) satisfying the Rex (see Rex [14, 15]) criteria for a minimum of five days; (ii) a negative or small positive zonal index (less than 50 units as suggested by Lupo and Smith [10]), must be identified on a time-longitude or Hovmöller diagram; (iii) conditions (i) and (ii) satisfied for 24 h after (before) onset (termination); (iv) the blocking event should be poleward of 35 N during its lifetime, and the ridge should have an amplitude of greater than 5 degrees latitude; and (v) blocking onset is determined to occur when condition (iv) and either conditions (i) or (ii) are satisfied, while (vi)termination is designated at the time the event fails condition (v) for a 24 h period or longer. This procedure is used to detect the blocking events at 500 hPa and defines the blocking duration using these start and end dates.

References

[1] Athar, H., Lupo, A.R., 2010. Scale and stability analysis of blocking events from 2002-2004: A case study of an unusually persistent blocking event leading to a heat wave in the Gulf of Alaska during August 2004. Adv. Met. 2010, Article ID 610263, 15 pages doi:10.1155/2010/610263.

[2] Dymnikov, V.P., Kazantsev, Y.V., Kharin, V.V., 1992. Information entropy and local Lyapunov exponents of barotropic atmospheric circulation. Izv. Atmos. Oceanic Phys. 28, 425-432.

[3] Dong, L., Colucci, S.J., 2005. The role of deformation and potential vorticity in southern hemisphere blocking events. J. Atmos. Sci. 62, 4043-4056.

[4] Haines, K., Holland, A.J., 1998. Vacillation cycles and blocking in a channel. Q. J. R. Meterol. Soc. 124, 873-897.

[5] Hansen, A.R., Sutera, A., 1993. A comparison between planetary-wave flow regimes and blocking. Tellus 45A, 281-288.

[6] Jensen, A.D., Lupo, A.R., 2013. Using enstrophy advection as a diagnostic to identify blocking regime transition. Q.J.R. Meterol. Soc. DOI: 10.1002/qj.2248.

[7] Jensen, A.D., Lupo, A.R., 2013. Using enstrophy-based diagnostics in an ensemble for two blocking events. Adv. Met.2013, Article ID 693859, 7 pages, 2013. doi:10.1155/2013/693859.

[8] Kalnay, E., Kanamitsu, M., Kistler, R., Collins, W., Deaven, D., Gandin, L., Iredell, M., Saha, S., White, G., Woollen, J., Zhu, Y., Leetmaa, A., Reynolds, R., Chelliah, M., Ebisuzaki, W., Higgins, W., Janowiak, J.,Mo, K.C., Ropelewski, C., Wang, J., Jenne, R., Joseph, D., 1996. The NCEP/NCAR 40-year reanalysis project. Bull. Amer. Meteor. Soc. 77, 437-471.

[9] Lejenas, H., Okland, H., 1983. Characteristics of Northern Hemisphere blocking as determined from a long time series of observational data. Tellus 35A, 350-362.

[10] Lupo, A.R., Smith, P.J., 1995. Climatological features of blocking anticyclones in the Northern Hemisphere. Tellus 47A, 439-456.

[11] Lupo, A.R., Mokhov, I.I., Dostoglou, S., Kunz, A.R., Burkhardt, J.P., 2007. The impact of the planetary scale on the decay of blocking and the use of phase diagrams and enstrophy as a diagnostic. Izv. Atmos. Oceanic Phys. 42, 45-51.

[12] Lupo, A.R., Mokhov, I.I., Akperov, M.G., Cherokulsky, A.V., Athar, H., 2012. A dynamic analysis of the role of the planetary and synoptic scale in the summer of 2010 blocking episodes over the European part of Russia. Adv. Meteor. 2012, Article ID 584257, 11 pages, doi:10.1155/2012/584257.

[13] Pedlosky, J., 1987. Geophysical Fluid Dynamics. Springer-Verlag, New York.

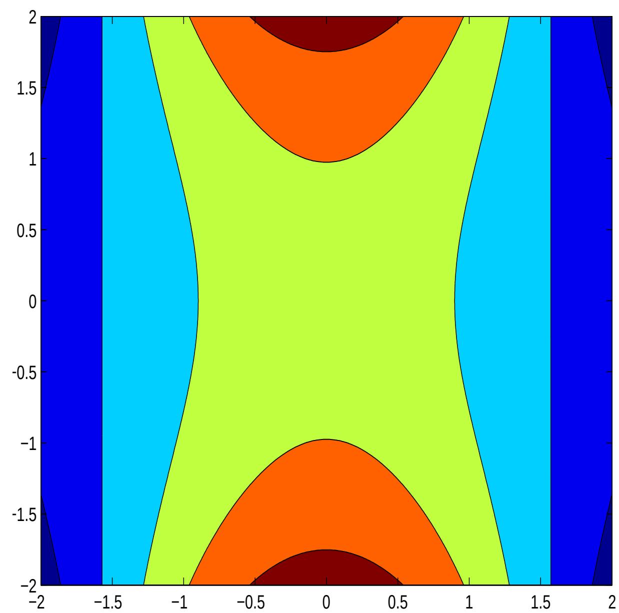

Figure A.1: Contours for the solution (10) of equation (9), with $A = k = 1$.

[14] Rex, D.F., 1950a. Blocking action in the middle troposphere and its effect on regional climate I: The Climatology of blocking action. Tellus 2, 196-211.

[15] Rex, D.F., 1950b. Blocking action in the middle troposphere and its effect on regional climate II: The Climatology of blocking action. Tellus 3, 275-301.

[16] Weiss, J., 1991. The dynamics of enstrophy transfer in two-dimensional hydrodynamics. Physica D, 273-294.

[17] Wiedenmann, J.M., Lupo, A.R., Mokhov, I.I., Tikhonova, E., 2002. The climatology of blocking anticyclones for the Northern and Southern Hemisphere: Block Intensity as a diagnostic. J. Climate 15, 3459-3473.

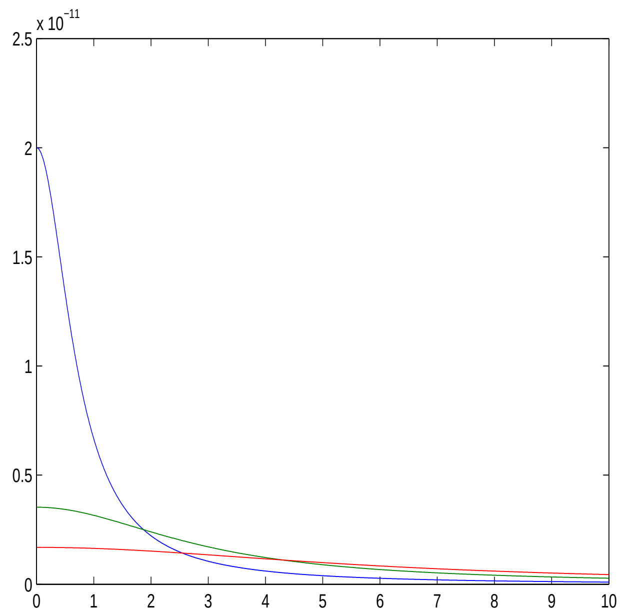

Figure A.2: Dispersion relation for $k = 1$ (blue), $k = 3$ (green), $k = 6$ (red) and $A = 1$.

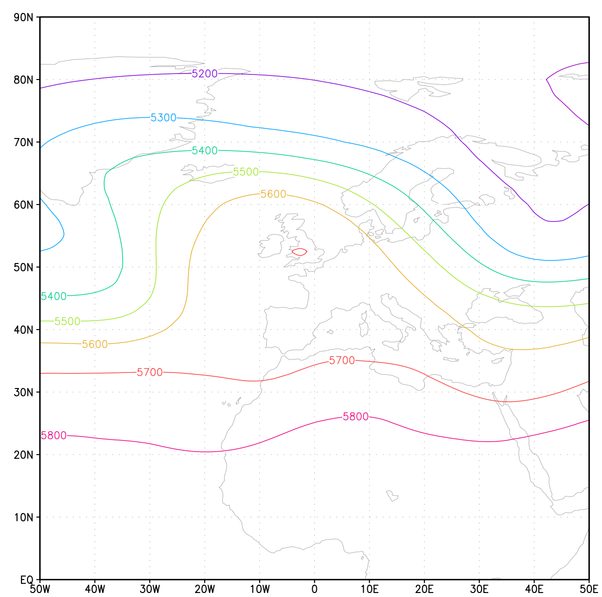

Figure A.3: Mean geopotential heights for 25 March-2 April 2012.

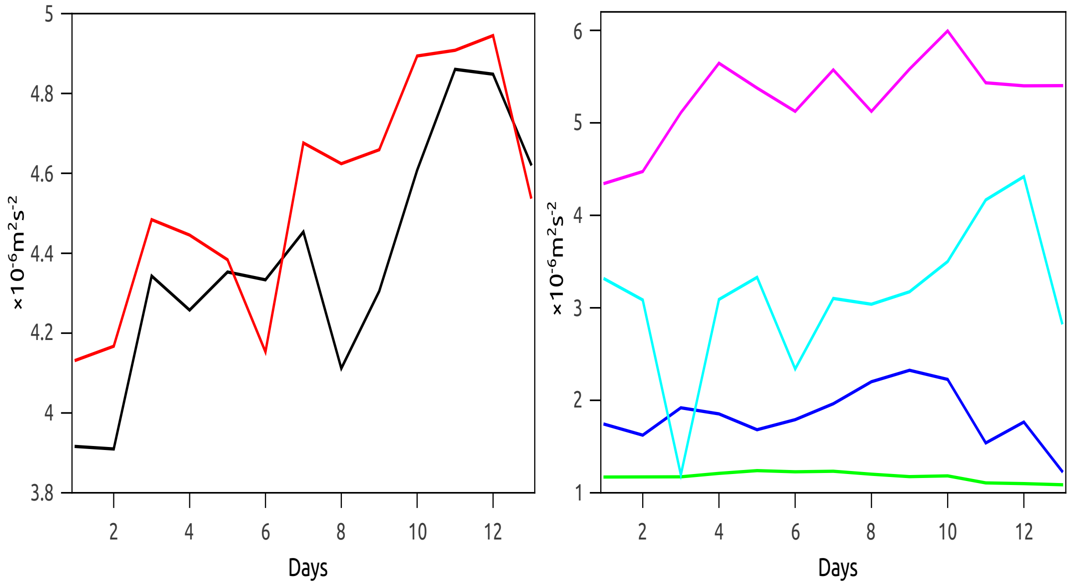

Figure A.4: Days for March 23-April 4. Left panel: IRE from equation (6) (red), IRE (black). Right panel: $u\beta$ (green), deformation (magenta), relative vorticity (cyan), geopotential height (blue).